Neuroscience xx (2006) xxx

PRESERVATION OF THE DIRECT AND INDIRECT PATHWAYS IN AN *IN VITRO* PREPARATION OF THE MOUSE BASAL GANGLIA

C. BEURRIER,* Y. BEN-ARI AND C. HAMMOND

INSERM, U29, Institut de Neurobiologie de la Méditerranée, Université de la Méditerranée, 163 route de Luminy, BP 13, 13273 Marseille cedex 09, France

Abstract—We have developed a slice preparation of the mouse basal ganglia which contains portions of the striatum, external pallidum, subthalamic nucleus and substantia nigra and the neocortex. This basal ganglia slice is unique in preserving functional direct and indirect connections between the striatum and the substantia nigra as well as interconnectivity between the globus pallidus and the subthalamic nucleus. We used fiber tract tracing studies and electrophysiological recordings to demonstrate the full functionality of these pathways. Deposits of 1,1′-dioctadecyl-3,3,3′,3′-tetramethylindocarbocyamine perchlorate in the different basal ganglia resulted in labeled fibers in each of their target nuclei. Confirming these results, electrical stimulation of the different nuclei elicited whole-cell recorded postsynaptic potentials in their target neurons with an appropriate pharmacological profile. Electrical and glutamate activation of the striatum evoked bursts of glutamatergic and GABAergic activities in whole-cell recorded nigral neurons indicating that the direct and indirect pathways are operative in this slice. It also showed that the responses evoked are not due to fibers en passant but to the activation of striatal cell bodies. These findings provide the first direct evidence for a preserved basal ganglia circuitry *in vitro* and make the basal ganglia slice a suitable preparation for analyzing the activity of the direct and indirect pathways in physiological and pathological conditions.

Key words: DiI, patch clamp, striatum, pallidum, subthalamic nucleus, substantia nigra.

The basal ganglia (BG) nuclei are a set of interconnected subcortical brain nuclei primarily involved in movements and motivational aspects of motor behavior (Crossman, 1987; Graybiel et al., 1994). The striatum is the major input structure of the BG since it receives excitatory afferents from nearly all cortical regions (McGeorge and Faull, 1989) whereas the substantia nigra pars reticulata (SNr) and the entopeduncular nucleus (EP, the homologue in rodents of the internal pallidal segment) are the output structures. Two main intrinsic pathways connect these input and output structures, the direct and indirect striato-nigral/entopeduncular pathways (Smith et al., 1998). The indirect pathway successively involves the globus pallidus (GP, homologue in rodents of the primate external pallidal segment), the subthalamic nucleus (STN) and the SNr (or the EP). Extracellular recordings performed on anesthetized rats showed that activation of the indirect pathway generates an excitation of SNr neurons via a disinhibitory process because the striato-pallidal and pallido-subthalamic neurons are GABAergic whereas the subthalamic ones are glutamatergic. In contrast the direct striato-nigral GABAergic pathway inhibits the tonic activity of SNr neurons (Maurice et al., 1999; Kolomiets et al., 2003). As a result, the indirect pathway counteracts the inhibitory influence exerted by the direct one on SNr neurons.

In working models of the BG, it is assumed that functional imbalance between the direct and indirect pathways underlies the motor disorders observed in BG pathologies (Albin et al., 1989; DeLong, 1990). In Parkinson's disease, the loss of dopaminergic innervation of the striatum, due to the degeneration of nigro-striatal dopaminergic neurons is responsible for this imbalance.

In vivo studies greatly contributed to our understanding of the normal and altered function of this network but are limited, as far as the cellular and molecular mechanisms underlying the network events are concerned. Slice experiments, which allow a better control of the external medium and recordings from identified structures and neurons, have indeed provided most of our present knowledge about the physiological mechanisms of neuronal plasticity, synaptic function and intrinsic oscillations. However, to date, standard BG slices contained two or three nuclei at best (Calabresi et al., 1991; Kita, 2001; Falkenburger et al., 2001; Cooper and Stanford, 2001; Hallworth and Bevan, 2005), thus reducing their utility for more integrative studies. Organotypic cultures, where up to three BG nuclei were co-cultivated, provided an interesting opportunity to propose that STN and GP neurons form a BG pacemaker loop (Plenz and Kitaï, 1999). However, this preparation used immature neurons and thus does not necessarily reflect the adult *in vivo* situation as it may favor the development of abnormal connections (Czubayko and Plenz, 2002).

To better understand the normal and pathological function of this complicated set of structures, we have developed an *in vitro* preparation of the direct and indirect BG pathways. To this aim, we performed 400 μm-thick para-

*Corresponding author. Tel: +33-491-82-81-10; fax: +33-491-82-81-01.
E-mail address: beurrier@inmed.univ-mrs.fr (C. Beurrier).

Abbreviations: BG, basal ganglia; BGS, basal ganglia slice; DiI, 1,1′-dioctadecyl-3,3,3′,3′-tetra-methylindocarbocyamine perchlorate; DPSPs, depolarizing postsynaptic potentials; EP, entopeduncular nucleus; EPSCs, excitatory postsynaptic currents; GP, globus pallidus; IPSCs, inhibitory postsynaptic currents; L-glu, L-glutamic acid; MSN, medium spiny neuron; NBQX, 2,3-dioxo-6-nitro-1,2,3,4-tetrahydrobenzoquinoxaline-7-sulfonamide; polyPSC, polysynaptic postsynaptic current; QX314, *N*-(2,6-dimethylphenylcarbamoylmethyl)triethylammonium bromi69; SNc, substantia nigra pars compacta; SNr, substantia nigra pars reticulata; STN, subthalamic nucleus; TH, tyrosine hydroxylase.

0306-4522/06$30.00+0.00
doi:10.1016/j.neuroscience.2006.02.029

sagittal slices of the mouse brain with different angles (from 0° to 20°) from the medial sagittal plane and checked the presence and functionality of the different components of the direct and indirect pathways by anatomical and electrophysiological techniques. We show that the best compromise is a 10° angle, which allows getting in the same slice, portions of four BG nuclei plus the cortex, functional direct and indirect connections between the striatum and the SNr, as well as part of the pallido-subthalamo-pallidal loop. This basal ganglia slice (BGS), which can be performed from control, lesioned or transgenic mice, will allow understanding the cellular mechanisms underlying the activity of the BG network in physiological and pathological conditions.

EXPERIMENTAL PROCEDURES

Slice preparation

All animal experiments were carried out in accordance with the European Communities Council Directive of 24 November 1986 (86/609/EEC). The experimental protocols were carried out in compliance with institutional ethical committee guidelines for animal research, and all efforts were made to minimize the number of animals used and their suffering. C57/Bl6 mice aged postnatal days 20–32 were killed by decapitation under halothane anesthesia and 400 μm-thick parasagittal slices were cut. They included part of the striatum, the GP, the STN and the SN and their main connections when cut at an angle of 10±2° (Fig. 1). This method generated one slice per hemisphere where most of BG nuclei and their connections were well preserved. For the slicing procedure, the solution contained (in mM) 110 choline, 2.5 KCl, 1.25 NaH_2PO_4, 7 $MgCl_2$, 0.5 $CaCl_2$, 25 $NaHCO_3$, 7 glucose. After a recovery period, we recorded the slices in a submersion-type chamber at room temperature with standard ACSF saturated with 95% O_2/5% CO_2 and containing (in mM) 126 NaCl, 3.5 KCl, 1.2 NaH_2PO_4, 1.3 $MgCl_2$, 2 $CaCl_2$, 25 $NaHCO_3$, 11 glucose. During the recovery period, we kept the slices in this solution supplemented with 250 μM kynurenic acid and 1 mM sodium pyruvate.

Electrophysiology

Cells were visualized with infrared-differential interference optics (Axioskop2, Zeiss, LePecq, France). We performed patch-clamp recordings in the whole cell configuration using the Digidata 1344A interface, the Multiclamp 700A amplifier and PClamp8 software (Axon Instruments, Foster City, CA, USA). For current-clamp recordings, patch electrodes (6–10 MΩ) contained (in mM): 120 K-gluconate, 20 KCl, 10 HEPES, 2 MgATP and 0.5 NaGTP, pH 7.2–7.4 (285–295 mOsm). For voltage-clamp recordings of nigral neurons, the pipette contained (in mM) either: 140 CsCl, 10 NaCl, 0.1 CaCl, 10 HEPES, 1 EGTA, 2 MgATP and 0.5 NaGTP or 120 Cs-gluconate, 13.6 CsCl, 10 HEPES, 1.1 EGTA, 0.1 CaCl, 2.5 MgATP and 0.3 NaGTP, pH 7.2–7.4 (285–295 mOsm). *N*-(2,6-dimethylphenylcarbamoylmethyl)triethylammonium bromi69 (QX314, 2 mM) was included to the CsCl solution to block postsynaptic sodium currents. The KGlu and CsCl pipette solutions gave a reversal potential for chloride equal to −48 and 0 mV, respectively. We used the CsGlu solution to measure spontaneous inhibitory and excitatory currents at the reversal potential for glutamatergic (+10 mV) and GABAergic (−60 mV) events respectively as already described in hippocampal neurons (Cossart et al., 2000).

Electrical stimulation was provided by custom-made bipolar electrodes positioned in the different nuclei under study (20–50 μs in duration, intensity from 6 to 80 V).

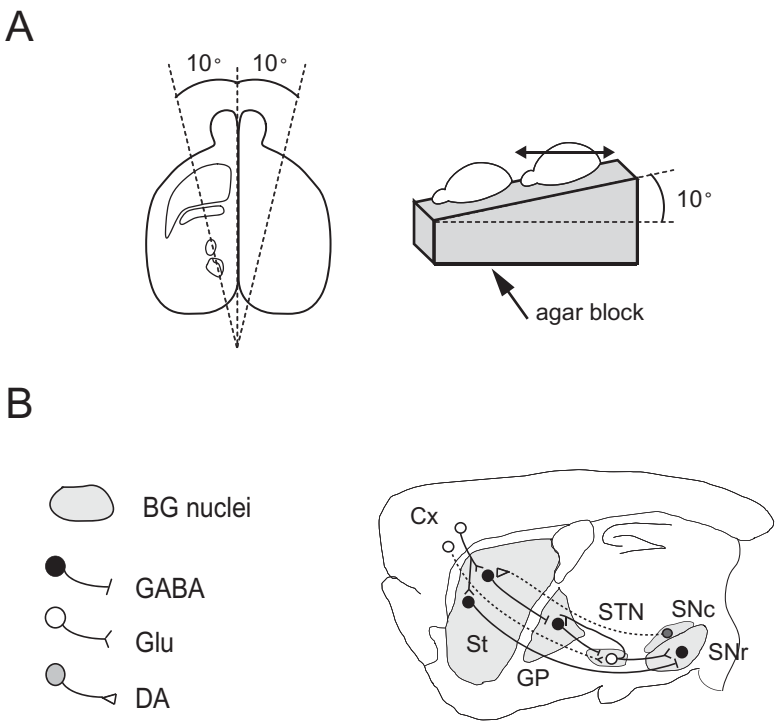

Fig. 1. The BG slice. (A) Scheme of the mouse brain seen from above with the estimated location of four of the BG nuclei. The two hemispheres are separated along the midline and glued to an agar block tilted at 10°. The double arrow represents the vibratome blade. (B) Scheme of the 10° slice showing the BG nuclei identified and the connections assessed. The two pathways represented with dotted lines are not present in the slice (see Results).

A glass electrode (tip diameter, 3–5 μm) was placed in the striatum and was used to evoke synaptic responses in nigral cells. This stimulating electrode was filled with 3 mM L-glutamic acid monosodium salt (L-glu) in extracellular solution and was connected to a picospritzer. L-Glu was ejected by pulses of 10 p.s.i. and 10–900 ms duration (increment: 50–100 ms). The synaptic bursts included in the analysis were the ones obtained with the minimal duration evoking a response. In some experiments the addition of Methylene Blue in the electrode solution enabled the spread of the stimulating solution to be visualized. All ejections were restricted to the striatum.

Data analysis

To isolate pharmacologically the GABAergic and glutamatergic pathways, we used blockers of the ionotropic glutamatergic and GABAergic transmissions, respectively. We stimulated the afferent structures at 0.1 Hz and analyzed the evoked synaptic responses with Mini-analysis software (Synaptosoft, v6.0.1). We considered the evoked synaptic potentials as monosynaptic on the basis of their constant latency over the sweeps, one trial consisting of 10–20 sweeps. Following afferent stimulation, neurons from a given nucleus within the same slice behaved consistently: they either presented a synaptic response or not. No attempt was made to identify areas within individual nuclei that might better respond to afferent stimulation. We considered a synaptic connection reliable when the stimulation of the afferent structure elicited a response in at least 90% of the slices.

The charge transfer of the polysynaptic responses observed in nigral cells after electrical or L-glu stimulation of the striatum was measured by integrating the area between the baseline and the evoked current trace using Origin 7.5 (OriginLab Corporation, Northampton, MA, USA). The charge transfer of the L-glu-evoked bursts (burst charge transfer) was compared with the charge transfer measured from recordings taken just before L-glu ejection (control charge transfer). The length of the period analyzed in control was equal to that of the L-glu-evoked synaptic burst. Charge transfer gives a good measure of the amount of synaptic inputs received by the cells as it takes into account the increase in the frequency of spontaneous post-synaptic currents and the development of tonic currents, both phenomena being observed in SNr cells after striatal L-glu stimulation.

The postsynaptic potentials or currents evoked by afferent stimulation illustrated in the figures represent the average of eight to 20 individual sweeps. Average values are presented as means$\pm$S.E.M. Statistical comparisons were performed with the Student's *t*-test.

Drugs

Drugs were prepared as concentrated stock solutions and diluted in ACSF for bath application or pressure ejection. Bicuculline, a selective $GABA_A$ receptor antagonist, and 2,3-dioxo-6-nitro-1,2,3,4-tetrahydrobenzoquinoxaline-7-sulfonamide (NBQX), an AMPA-kainate receptor antagonist, were used at a concentration of 10 μM. These agents, plus QX314, were purchased from Tocris-Fisher Bioblock Scientific.

1,1′-Dioctadecyl-3,3,3′,3′-tetra-methylindocarbocyamine perchlorate (DiI) experiments

Mice (P20–22) were anesthetized with chloral hydrate (7%) and intracardially perfused with 4% paraformaldehyde. Brains were post-fixed by immersion for 2–4 weeks in the cold fixative solution containing 4% paraformaldehyde and cut into 400-μm parasagittal sections with an angle of 10$\pm$2°. The slices used for axon tracing experiments were prepared exactly as those used for electrophysiological recordings (Fig. 1). We injected small amounts of DiI (Interchim, France) crystals diluted in ethanol in one nucleus of the BG. Slices were then incubated in the fixative solution at 32 °C for 2–3 weeks, counterstained with green fluorescent Nissl stain (Molecular Probes), coverslipped and examined with a fluorescence (Nikon Eclipse E800) and a confocal (Olympus Fluoview-500) microscope. To study the projection of the GP to the STN, a hemitransection rostral to the GP was performed 15 days before mice perfusion to ensure degeneration of cortico-subthalamical fibers that could be labeled by the DiI injection in the GP. Anesthetized mice were placed in a stereotaxic apparatus. A knife blade was lowered 4.9 mm from the skull surface and moved medio-laterally to cut fibers rostral to GP at anteriority 1.5 from the bregma.

Immunohistochemistry

In order to visualize the trajectory of nigro-striatal dopaminergic axons in the BGS, immunocytochemistry of tyrosine hydroxylase (TH) was performed in 75 μm-thick, 10°- tilted parasagittal slices and in horizontal slices. Sections were blocked by 2% normal goat serum (Abcys) in PBS containing 0.3% Triton X-100 for 30 min, and then incubated for 12 h with anti-TH monoclonal antibody (Chemicon International) at a dilution of 1:500 or 1:1000. After the sections had been washed with PBS, they were incubated for 1 h 30 with anti-mouse IgG secondary antibody (Tebu) at a dilution of 1:300. Sections were washed with PBS and incubated for 1 h 30 in Cy3-conjugated streptavidin (Jackson). They were mounted in fluoromount (Euromedex), coverslipped and examined with a confocal microscope (Olympus Fluoview-500).

RESULTS

In the 10° tilted parasagittal slice (Fig. 1A), portions of all BG nuclei were identified except for the EP. We checked the presence and functionality of the connections between each of the individual BG nuclei present in the slice (Fig. 1B). In addition to these pathways, which are intrinsic to the BG network, we also tested for the presence of the cortical entries to the BG: the cortico-striatal and the cortico-subthalamic pathways. We will present these results first. Two methods were used to check a connection: we visualized specific pathways using the axonal tracer DiI, then tested their functionality by stimulating the afferent structure and recording the synaptic response in the target nucleus. For technical reasons, DiI and electrophysiological experiments were conducted in different slices but cut exactly the same way (Fig. 1A). We then demonstrated the full functionality of the direct and indirect pathways by showing that electrical or pharmacological activation of the striatum evokes direct and indirect responses in the SNr.

Cortical inputs to BG

The two main BG nuclei that receive glutamatergic cortical inputs are the striatum and the STN (Afsharpour, 1985; McGeorge and Faull, 1989). We injected DiI crystals either over the whole cortex or in a restricted frontal area (Fig. 2A, B). Labeled corticofugal axons formed numerous bundles running radially through the whole striatum, reproducing the well-known striped appearance of this structure (n=15/15 slices) (Fig. 2A). The functionality of the connection was then assessed at the electrophysiological level. Neurons recorded in the striatum were identified as medium spiny neurons (MSNs) on the basis of their electrophysiological features (Wilson and Groves, 1981; Kita et al., 1985; Stern et al., 1997; Koos and Tepper, 1999).

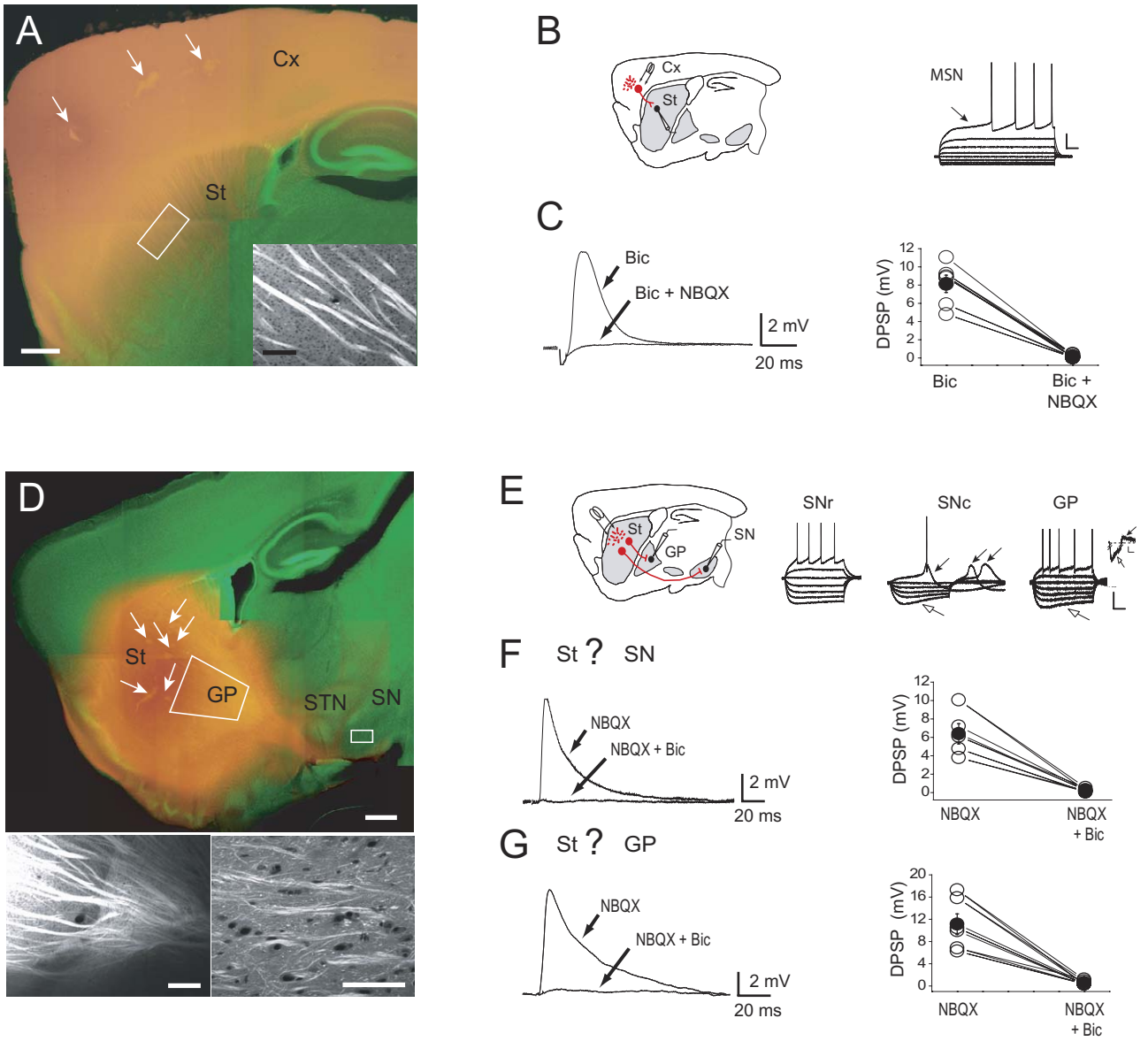

Fig. 2. The cortico-striatal, the direct striato-nigral and the striato-pallidal connections. (A) Computer-generated overlays of DiI-labeled axons and green fluorescent Nissl counterstain after DiI injections (white arrows) in the cortex (Cx, scale bar=500 μm). The inset shows a confocal view of the labeled fluorescent axons in the striatum (St, scale bar=100 μm). In this and subsequent figures, the rostral pole corresponds to the left side of the image. (B) Left, schematic illustrations of DiI injection (red dots), stimulation and recording sites in the BGS. Right, membrane responses to intracellular current pulses allowed the identification of MSN (V_m=−80 mV, arrow indicates the ramp depolarization). Calibration bars: 20 mV, 50 ms. (C) Pharmacology of DPSP for individual neurons (left) and for all the neurons recorded (right) in the St after cortical stimulation (V_m=−80 mV). (D) Computer-generated overlays of DiI labeled axons and green fluorescent Nissl counterstain after DiI injections (white arrows) in the striatum (scale bars=500 μm). The insets show confocal views of labeled axons in the GP (left, scale bar=200 μm) and the SN (right, scale bar=50 μm). (E) Left, schematic illustrations of DiI injection, stimulation and recording sites in the BGS. Right, membrane responses of nigral (SNr, SNc) and pallidal (GP) cells to current injections (calibration bars: 20 mV and 100 ms). The SNr cell (V_m=−70 mV) showed almost linear membrane responses while the SNc cell (V_m=−60 mV) displayed a pronounced time- and voltage-dependent sag of the membrane potential upon hyperpolarization (unfilled arrow) and robust depolarizing rebounds (black arrows). The GP neuron (V_m=−75 mV) exhibited a time- and voltage-dependent sag of the membrane potential (unfilled arrow). The inset shows the membrane response to the most negative current pulse with the middle part of the trace deleted to highlight the time- and voltage-dependent sag of the membrane potential (unfilled arrow) and the rebound depolarization (black arrow) (calibration bars are 5 mV and 200 ms). (F, G) Pharmacology of the DPSPs for individual neurons (left) and for all the neurons recorded (right) in the SN (F, V_m=−70 mV) and GP (G, V_m=−75 mV) after striatal stimulation. For interpretation of the references to color in this figure legend, the reader is referred to the Web version of this article.

MSNs (n=11) were silent at rest (V_{rest}=−74.1±0.7 mV, −76.5 to −70.0 mV, n=10), showed a delay to fire the first action potential when depolarized by positive current injection and a strong inward rectification at hyperpolarized potentials (Fig. 2B, right). Electrical stimulation of the cortex in the presence of bicuculline elicited a depolarizing

postsynaptic potential (DPSP) in MSNs (V_m=−80 mV, n=8 cells, seven slices). NBQX fully blocked this response (n=6 cells, six slices) (Fig. 2C). Thus, functional glutamatergic cortico-striatal connections are present in the BGS.

The second main target of the cortex is the STN. After deposit of DiI in the cortex, the fibers did not enter the STN even though the internal capsule and peduncles were labeled (n=10/12 slices, not shown). Indeed, cortical stimulation in the presence of bicuculline consistently failed to evoke DPSPs in STN neurons, although both striatal and internal capsule stimulations did. These results suggest that even though the complete cortico-subthalamic pathway might not be present in the slice, cortical fibers passing through the striatum and projecting to the STN were still able to release glutamate and evoke a synaptic response in STN neurons.

Intrinsic BG connections

The input structure of the BG network, the striatum, is connected to the output structures, the SNr and the EP, by a direct GABAergic striato-nigral pathway (Bevan et al., 1994), and an indirect one composed of the GABAergic striato-pallidal (Chang et al., 1981), the GABAergic pallido-subthalamic (Van der Kooy et al., 1981) and the glutamatergic subthalamo-nigral (Chang et al., 1984) connections. As the EP was absent in the BGS, we focused on the SN. In addition to the direct and indirect pathways, we also tested the glutamatergic subthalamo-pallidal (Kanazawa et al., 1976; Kita and Kitai, 1987) and the dopaminergic nigro-striatal (Freund et al., 1984) connections (Fig. 1B).

The direct striato-nigral connection. After striatal injection, DiI-labeled fibers run rostro-caudally to the peduncles before entering into the SN (n=7/7 slices) (Fig. 2D). We recorded two types of nigral neurons in the BGS. Their electrophysiological features identified the first group as GABAergic SNr neurons and the second group as dopaminergic substantia nigra pars compacta (SNc) neurons (Grace and Onn, 1989; Richards et al., 1997). SNr neurons (n=23) spontaneously fired at higher frequency (11.8±1.5 vs. 0.8±0.1 Hz, P<0.01), had narrow action potentials (0.90±0.04 vs. 2.44±0.13 ms, P<0.001) and did not display large rectification currents compared with SNc neurons (n=5) (Fig. 2E, right). Among the recorded cells, SNr neurons prevailed because we preferentially recorded from this area. Both types of SN cells displayed synaptic responses following striatal stimulation confirming the presence of functional striato-nigral connections (n=9 cells, 7 slices). DPSPs evoked in the presence of NBQX were blocked by bicuculline (V_m=−70 mV, n=5 cells, 5 slices) (Fig. 2F), showing that they were mediated by $GABA_A$ receptor activation.

The striato-pallidal connection. Striatal injection of DiI also led to extensive labeling of the GP. DiI-labeled striatofugal axons formed several high-density bundles passing rostro-caudally through the GP (n=10/10 slices) (Fig. 2D). Thin perpendicular axon collaterals clearly delineated the boundary between GP and striatum. Most GP neurons (n=26/33) fired spontaneously at a mean frequency of 14.6±2.6 Hz (1.9–57.1 Hz). In some cells (n=26/33), negative current pulses revealed a membrane sag and a depolarizing rebound (Fig. 2E, right) suggesting the presence of the inward rectifier current, I_h and the low voltage-activated calcium conductance, I_T. Electrophysiology confirmed the morphological data as striatal stimulation triggered DPSPs in GP neurons (NBQX, V_m=−75 mV, n=14 cells, 10 slices) that completely disappeared after adding bicuculline to the bath (n=6 cells, 6 slices) (Fig. 2G).

The pallido-subthalamic loop. GP and STN are reciprocally connected (Van der Kooy et al., 1981; Kita and Kitai, 1987). To properly isolate the pallido-subthalamic connection, we eliminated cortical fibers passing through the GP 15 days prior to DiI injection in the GP (see Experimental Procedures and Fig. 3A). Several DiI-positive fibers coursed rostro-caudally leading to dense labeling of the STN (n=7/7 slices) (Fig. 3A). Most STN neurons were quiescent (n=26/39, V_{rest}: −54.9±0.8 mV, −44.9 to −64.0 mV). The remaining neurons (n=13/39) spontaneously fired at 6.0±2.1 Hz (1.0–18.9 Hz). Injection of current steps into cells revealed a membrane sag as well as a depolarizing rebound, suggesting the presence of I_h and I_T (n=34/41) (Fig. 3B, right). Stimulating the GP in the presence of CNQX triggered a $GABA_A$ receptor-mediated DPSP in STN neurons (V_m=−70 mV, n=20 cells, 13 slices) that was fully abolished by bicuculline (n=13 cells, 10 slices) (Fig. 3C).

Injection of the tracer in the STN (Fig. 3D, E) gave rise to densely packed DiI-positive fibers coursing toward GP (n=16/16 slices). Supporting DiI results, STN stimulation in the presence of bicuculline triggered AMPA-receptor mediated DPSPs in GP neurons (V_m=−75 mV, n=34 cells, 24 slices) that were blocked by NBQX (n=12 cells, 12 slices) (Fig. 3F).

The subthalamo-nigral pathway. After injection of DiI in the STN (Fig. 3D), labeled fibers crossed the upper branch of the cerebral peduncles and entered into the SN via its rostral pole (n=13/16 slices) (Fig. 3D). Part of this pathway was functional as electrical STN stimulation evoked DPSPs in both types of SN neurons in the presence of bicuculline (V_m=−70 mV, n=16 cells, 14 slices). NBQX greatly reduced these DPSPs (n=13 cells, 13 slices) (Fig. 3G).

The ascending nigro-striatal dopaminergic pathway. Immunolabeling showed that TH-positive SNc (A9) neurons and fibers are present in the BGS. In particular, intense fiber labeling was observed in the STN and striatum. However, the projection is not included in its full extent in the BGS. Horizontal slices revealed clearly that TH-positive fibers course medially to the STN (medial forebrain bundle) and are thus at that level medial to the BGS (data not shown).

The direct and indirect pathways

A major feature of the BG network is the convergence of the direct GABAergic and the indirect glutamatergic pathways onto single neurons of the output structures (Kita,

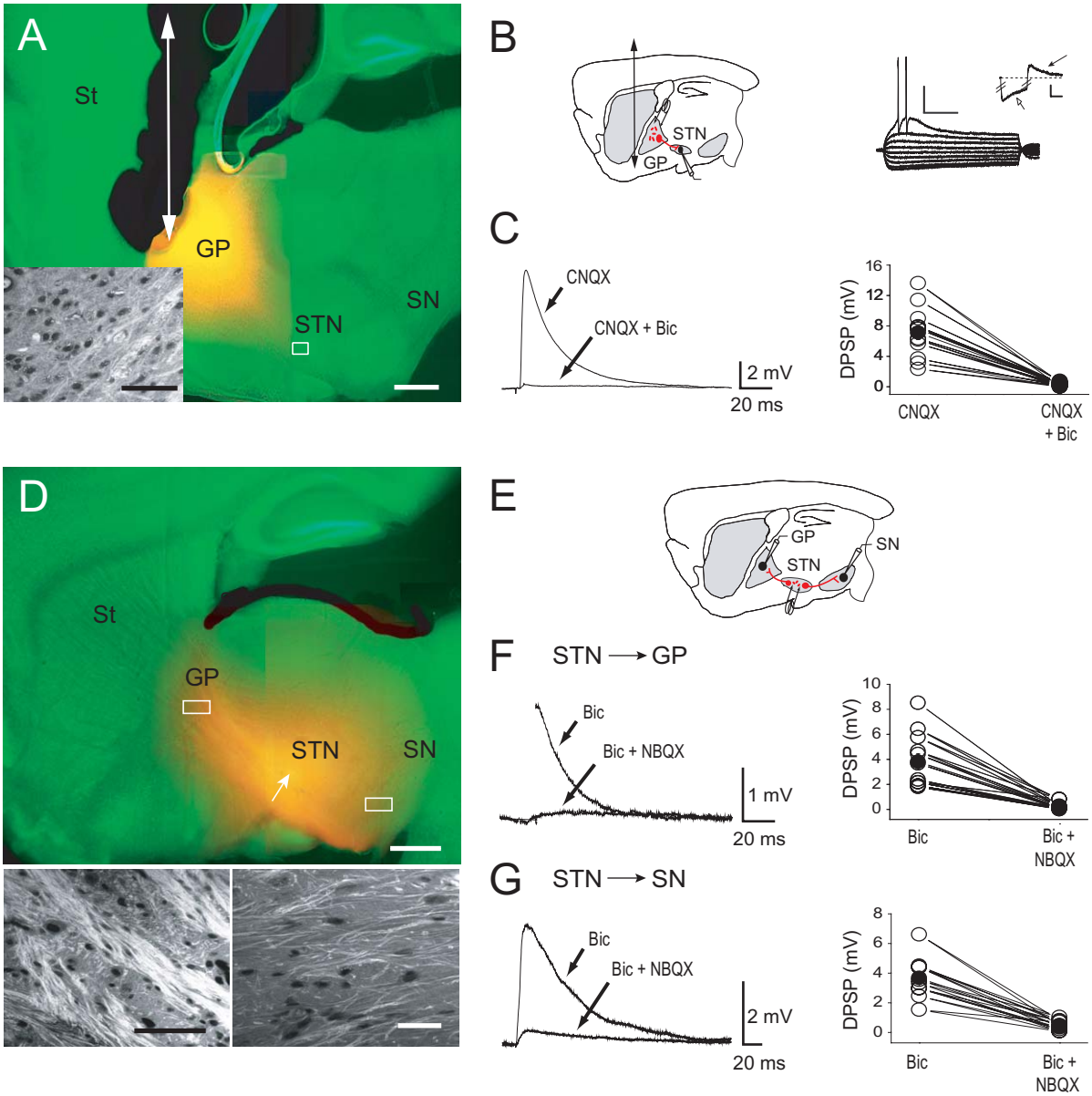

Fig. 3. The pallido-subthalamic loop and the subthalamo-nigral connection. (A, D) Computer-generated overlays of DiI-labeled axons and green fluorescent Nissl counterstain after DiI injections in the GP (A) and the STN (D) (white arrows) (scale bars=500 μm). The insets show a confocal view of the labeled axons in the STN (A, scale bar=100 μm), the GP (D left, scale bar=50 μm) and the SN (D right, scale bar=50 μm). The transversal arrows in A and B indicate the hemitransection done *in vivo* to make corticofugal axons degenerate. (B, Left, E) Schematic illustrations of DiI injection, stimulation and recording sites in the BGS. (B) Right, membrane responses of a STN neuron to current steps (V_m=−70 mV, calibration bars: 20 mV and 100 ms). The inset shows the response to the most negative current pulse with the middle part of the trace deleted to highlight the I_h-dependent sag of membrane potential (unfilled arrow) and the rebound depolarization (black arrow) (calibration bars are 4 mV and 200 ms). (C, F, G) Pharmacology of the DPSPs for individual neurons (left) and for all the neurons recorded (right) in the STN after GP stimulation (C, V_m=−70 mV), in the GP after STN stimulation (F, V_m=−75 mV) and in the SN after STN stimulation (G, V_m=−70 mV).

1994; Bevan et al., 1994) (Fig. 4A). To date, such polysynaptic responses have been observed *in vivo* only, since their activation require a preserved BG network (Kolomiets et al., 2003). If the BG circuitry were somehow preserved in the BGS, we should be able to observe such direct and indirect responses in SNr neurons. We triggered them by striatal activation since cortical stimulation failed to induce action potentials in MSNs, evoked DPSPs remaining subthreshold (see Cortical inputs to BG and Calabresi et al., 1999). Striatal stimulation evoked a polysynaptic postsynaptic current (polyPSC) in 28 of 31 voltage clamped SNr cells (V_h=−70 mV, n=22 slices) (Fig. 4B). Part of the polyPSC was mediated by AMPA receptors as NBQX decreased its charge transfer by 54%, from 6.39±0.91–2.93±0.68 pC/s (n=12 cells, 12 slices, P<0.01). The subsequent addition of bicuculline almost completely suppressed the NBQX-insensitive current (from 2.93±0.68–0.24±0.04 pC/s, n=12 cells, 12 slices, P<0.001)

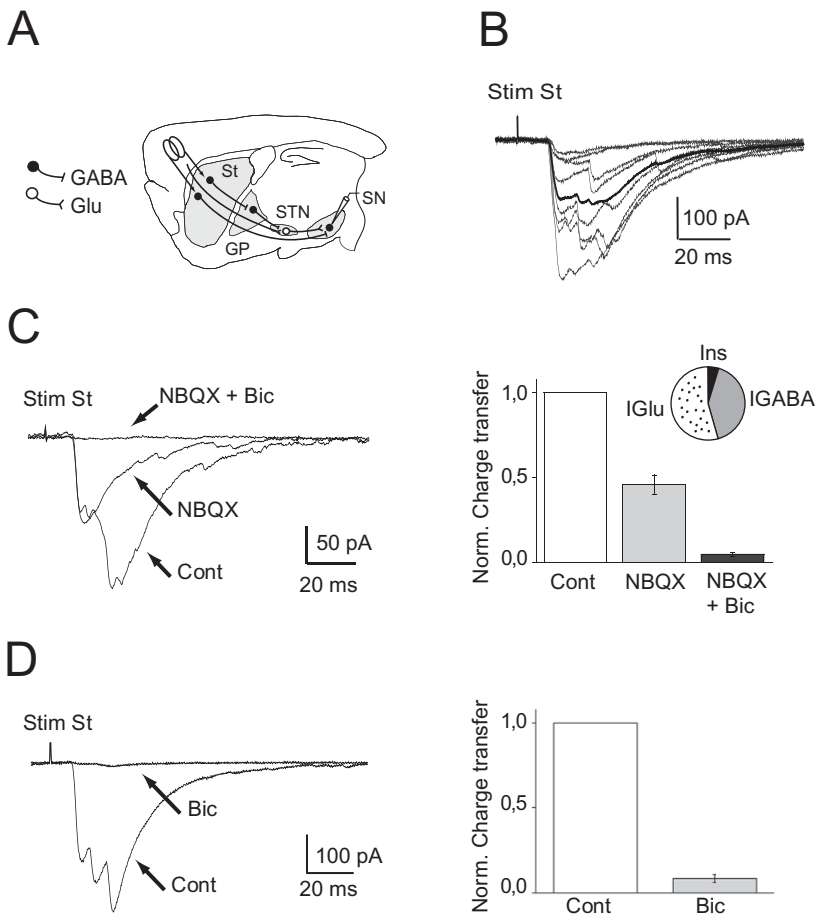

Fig. 4. Convergence of the direct and indirect pathways onto single SNr neurons. (A) Schematic illustration of the connections tested. (B) Voltage clamp recording ($V_h = -70$ mV) from a SNr cell during stimulation of the striatum (Stim St). The gray traces represent eight superimposed individual sweeps and the black trace represents the average of the eight sweeps. (C) Polysynaptic current evoked in a SNr cell clamped at −70 mV before (Cont), during application of 10 μM NBQX and after addition of 10 μM bicuculline (NBQX+Bic) (left). Summarizing graph of the polyPSC charge transfer in control, NBQX and after NBQX-bicuculline applications ($n=12$). The proportion of glutamatergic (IGlu), GABAergic (IGABA) and non-specific (Ins) current is indicated on the pie (right). (D) PolysPSC evoked in a SNr cell clamped at −70 mV before (Cont) and after application of 10 μM bicuculline (left). Summarizing graph of the normalized polyPSC charge transfer in control and bicuculline conditions ($n=6$ cells) (right).

(NBQX+Bic, Fig. 4C). These experiments indicate that both GABAergic and glutamatergic transmissions participated to the polyPSC evoked in SNr cells. The bicuculline sensitive current was likely due to the activation of the direct GABAergic pathway while activation of indirect polysynaptic pathways, which include glutamatergic synapses, would be responsible for the NBQX-sensitive current. These polysynaptic pathways could be the hyperdirect one (cortico-subthalamo-nigral) and/or the indirect one (striato-pallido-subthalamo-nigral) (Fig. 4A). Even though the complete cortico-subthalamic pathway is not preserved in the BGS, we showed above that stimulation of cortical axons passing through the striatum evoked glutamatergic responses in STN neurons (see Cortical inputs to BG).

We used bicuculline to discriminate between these two possibilities since the hyperdirect pathway is formed exclusively of glutamatergic synapses. Bicuculline almost completely blocked the polyPSC evoked in SNr cells by stimulation of the striatum. The mean polyPSC charge transfer was reduced by 94% (from 4.79±1.3–0.3±0.03 pC/s, $n=6$ cells, 5 slices, $P<0.05$) (Fig. 4D). This suggested that the glutamatergic component of the polyPSC resulted from the activation of the indirect striato-pallido-subthalamo-nigral pathway.

It is tempting from the above experiments to conclude that the BGS preserved intact connections between the input structure, the striatum, and the output structure, the SNr. However, neither electrical stimulation nor axon tracing enables us to conclude that the stimulated or stained axons are still attached to their cell bodies. To ascertain that functional synaptic units (the cell bodies, their axons and their synaptic targets) are preserved in the BGS, we repeated the same experiments than above but we replaced the electrical stimulation of the striatum by local applications of glutamate (L-glu) so that cell bodies were activated but axons were not. As striatal MSNs do not fire action potential easily because of their negative membrane potential, we first checked the effect of L-glu ejection on MSNs activity. We found that 3 mM L-glu consistently elicited a burst of action potentials in MSNs at their resting

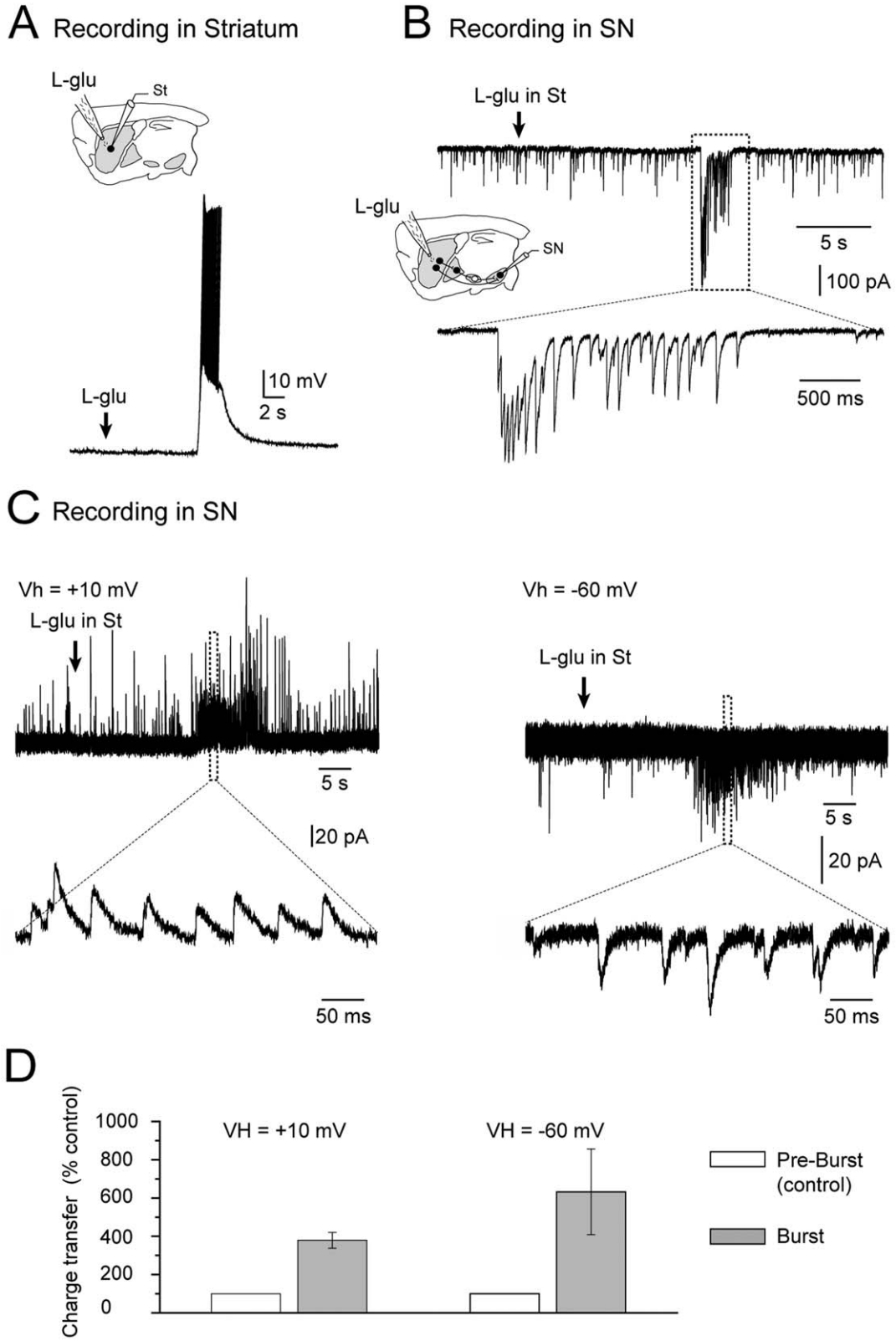

Fig. 5. Direct and indirect responses recorded in nigral cells after striatal glutamate stimulation. (A) An example of a burst of action potentials recorded from a MSN in response to glutamate (L-glu) application in the striatum (arrow, pulse duration: 40 ms). The MSN membrane potential is −75 mV (no current injected). (B) L-Glu stimulation in the striatum (arrow, pulse duration: 40 ms) evoked a burst of synaptic activities in a SNr cell recorded in voltage clamp mode with a CsCl-filled electrode (V_h=−70 mV). (C) Traces from a SNr cell recorded in voltage clamp mode with a CsGlu-filled electrode showing a burst of IPSCs at +10 mV and a burst of EPSCs at −60 mV after L-glu application in the striatum (arrows, pulse duration at +10 mV: 400 ms and at −60 mV: 200 ms). The enlarged traces show the slow kinetics of the decay phase of the IPSCs (left) compared with that of EPSCs (right). (D) Summary graph of the synaptic charge transfer calculated before the L-glu striatal application (Pre-burst) and during the burst for all the SNr cells recorded with a CsGlu-filled electrode (n=5 cells).

membrane potentials (Fig. 5A). Such L-glu ejection generated within a few seconds (from 10.03–38.18 s) a burst of synaptic activity (duration: 6.33±1.52 s, from 2.52–10.06 s) in five of six SNr neurons recorded in the voltage-clamp mode (V_h=−70 mV, n=5 slices) (Fig. 5B). It was often necessary to move the L-glu-filled electrode several times before finding the striatal area connected to the SNr cell recorded. The synaptic charge transfer was increased during the burst by 714% (from 23.58±5.72–192.12±37.11 pC/s, $P<0.05$, n=5 cells, 5 slices). The CsCl-filled electrode used in these experiments did not allow distinguishing between GABAergic and glutamatergic events as the reversal potential for both chloride and cationic ions was equal to 0 mV. For this reason we recorded some cells with a CsGlu-filled electrode to measure inhibitory (IPSCs) and excitatory (EPSCs) postsynaptic currents at the reversal potential for glutamatergic (+10 mV) and GABAergic (−60 mV) events, respectively. In this condition, L-glu stimulation evoked a burst of IPSCs at +10 mV (burst duration: 7.41±1.97 s, from 2.53–11.79 s, n=5 cells, 5 slices) and a burst of EPSCs at −60 mV (burst duration: 8.91±2.03 s, from 3.27–14.02 s, n=5 cells, five slices) (Fig. 5C). Two cells displayed a response at +10 mV but not at −60 mV (the reverse was never observed) and were not included in the analysis. The delay between the L-glu ejection in the striatum and the synaptic burst evoked in SNr neurons was quite variable (from 9.98–20.13 s at +10 mV and from 13.82–30.86 s at −60 mV). This variability may be due to the absence of rigorous somatotopic organization of the striatal efferences. The synaptic charge transfer was increased during the burst by 295% of control at +10 mV (from 51.1±8.74–201.85±49.62 pC/s, $P<0.05$) and by 302% at −60 mV (from 15.43±6.67–62.02±20.3 pC/s, P=0.07) (Fig. 5D). The lack of statistical significance at −60 mV is explained by the variability in the charge transfer of the evoked synaptic bursts. These results suggested that the neurons forming the direct and indirect pathways were preserved in the BGS.

DISCUSSION

To our knowledge, this is the first description of a mouse slice preparation where four different BG nuclei plus the cortex are maintained with most of their connections. Even though the BGS does not contain the entirety of the BG nuclei and pathways, the neuronal populations and connections preserved are sufficient to reproduce responses *in vitro* that are generated by the BG network *in vivo*. The glutamatergic and GABAergic responses obtained in SNr neurons after electrical and L-glu stimulation of the striatum suggest that both the direct and indirect pathways are present and functional in the BGS. However, we cannot completely rule out the participation of other pathways to these responses. We think that the BGS is a suitable preparation to study information processing all the way from the input (striatum) down to the output (SNr) structures of the BG network.

One BG nucleus, the EP, and two pathways, the hyperdirect cortico-subthalamic and the dopaminergic nigro-striatal pathways are absent in the BGS. Morphological results suggested that the cortico-subthalamic pathway stems out from the pyramidal tract and originates mainly from M1 cortical neurons in contrast to cortico-striatal neurons that arise from the entire cortical mantle (Wilson, 1987; Cowan and Wilson, 1994; Parent and Hazrati, 1995; Romanelli et al., 2005). This would explain why cortico-striatal connections are present in the BGS whereas cortico-subthalamic ones are not and why the stimulation of the internal capsule evoked glutamatergic DPSPs in STN neurons. Immunohistochemical results showed that the BGS does not contain the entire course of the dopaminergic ascending axons. TH-positive fibers were observed only rostrally to the STN in their course toward the striatum. However, the striatum and to a lesser extent the STN showed dense immunocytochemical labeling. Thus, the BGS is not a dopamine-deficient BG system.

Previous *in vitro* acute preparations of the BG allowed studying individual connections only, such as the cortico-striatal (Calabresi et al., 1991; Cepeda et al., 1993), the striato-pallidal (Kita, 2001; Cooper and Stanford, 2001), the subthalamo-nigral (Falkenburger et al., 2001) and more recently the pallido-subthalamic and subthalamo-pallidal connections (Hallworth and Bevan, 2005; Loucif et al., 2005). Although fundamental observations have been made in these preparations, the connectivity was restricted in most of the cases to two BG nuclei. The angle of 10° that we chose for the BGS was the best compromise for having in the same parasagittal slice significant parts of the rostral and caudal BG nuclei together with the neurons participating in the direct and indirect pathways.

It is currently believed that abnormal processing of cortical inputs through the striatofugal systems is involved in hyper and hypokinetic disorders. In particular, an imbalance between the direct and indirect pathways has been suspected to underlie the dyskinesia characteristics of Parkinson's disease (degeneration of dopaminergic neurons), ballism (STN lesion) or dystonia (unknown origin) (Albin et al., 1989; DeLong, 1990). By offering the unique opportunity to apprehend these aspects in a simplified but functional preparation from control, lesioned and/or transgenic mice, the BGS will help contributing to the comprehension of information processing performed by the BG network.

Acknowledgments—We thank P. Tosetti, J.-L. Gaiarsa and A. Barth for helpful comments on the manuscript and H. Becq and C. Lopez for technical assistance. This work was supported by grants from Fondation pour la recherche médicale (C.B.) and Fondation de France.

REFERENCES

Afsharpour S (1985) Topographical projections of the cerebral cortex to the subthalamic nucleus. J Comp Neurol 236:14–28.

Albin RL, Young AB, Penney JB (1989) The functional anatomy of basal ganglia disorders. Trends Neurosci 12:366–375.

Bevan MD, Bolam JP, Crossman AR (1994) Convergent synaptic input from the neostriatum and the subthalamus onto identified nigrothalamic neurons in the rat. Eur J Neurosci 6:320–334.

Calabresi P, Centonze D, Gubellini P, Marfia GA, Bernardi G (1999) Glutamate-triggered events inducing corticostriatal long-term depression. J Neurosci 19:6102–6110.

Calabresi P, Mercuri NB, De MM, Bernardi G (1991) Involvement of GABA systems in feedback regulation of glutamate-and GABA-mediated synaptic potentials in rat neostriatum. J Physiol 440: 581–599.

Cepeda C, Buchwald NA, Levine MS (1993) Neuromodulatory actions of dopamine in the neostriatum are dependent upon the excitatory amino acid receptor subtypes activated. Proc Natl Acad Sci U S A 90:9576–9580.

Chang HT, Kita H, Kitai ST (1984) The ultrastructural morphology of the subthalamic-nigral axon terminals intracellularly labeled with horseradish peroxidase. Brain Res 299:182–185.

Chang HT, Wilson CJ, Kitai ST (1981) Single neostriatal efferent axons in the globus pallidus: a light and electron microscopic study. Science 213:915–918.

Cooper AJ, Stanford IM (2001) Dopamine D2 receptor mediated presynaptic inhibition of striatopallidal GABA(A) IPSCs in vitro. Neuropharmacology 41:62–71.

Cossart R, Hirsch JC, Cannon RC, Dinoncourt C, Wheal HV, Ben-Ari Y, Esclapez M, Bernard C (2000) Distribution of spontaneous currents along the somato-dendritic axis of rat hippocampal CA1 pyramidal neurons. Neuroscience 99:593–603.

Cowan RL, Wilson CJ (1994) Spontaneous firing patterns and axonal projections of single corticostriatal neurons in the rat medial agranular cortex. J Neurophysiol 71:17–32.

Crossman AR (1987) Primate models of dyskinesia: the experimental approach to the study of basal ganglia-related involuntary movement disorders. Neuroscience 21:1–40.

Czubayko U, Plenz D (2002) Fast synaptic transmission between striatal spiny projection neurons. Proc Natl Acad Sci U S A 99: 15764–15769.

DeLong MR (1990) Primate models of movement disorders of basal ganglia origin. Trends Neurosci 13:281–285.

Falkenburger BH, Barstow KL, Mintz IM (2001) Dendrodendritic inhibition through reversal of dopamine transport. Science 293:2465–2470.

Freund TF, Powell JF, Smith AD (1984) Tyrosine hydroxylase-immunoreactive boutons in synaptic contact with identified striatonigral neurons, with particular reference to dendritic spines. Neuroscience 13:1189–1215.

Grace AA, Onn SP (1989) Morphology and electrophysiological properties of immunocytochemically identified rat dopamine neurons recorded in vitro. J Neurosci 9:3463–3481.

Graybiel AM, Aosaki T, Flaherty AW, Kimura M (1994) The basal ganglia and adaptive motor control. Science 265:1826–1831.

Hallworth NE, Bevan MD (2005) Globus pallidus neurons dynamically regulate the activity pattern of subthalamic nucleus neurons through the frequency-dependent activation of postsynaptic GABAA and GABAB receptors. J Neurosci 25:6304–6315.

Kanazawa I, Marshall GR, Kelly JS (1976) Afferents to the rat substantia nigra studied with horseradish peroxidase, with special reference to fibres from the subthalamic nucleus. Brain Res 115:485–491.

Kita H (1994) Physiology of two disynaptic pathways from the sensorimotor cortex to the basal ganglia output nuclei. In: . In: The basal ganglia IV (Percheron G, McKenzie JS, Feger J, eds), pp 263–276. New York: Plenum Press.

Kita H (2001) Neostriatal and globus pallidus stimulation induced inhibitory postsynaptic potentials in entopeduncular neurons in rat brain slice preparations. Neuroscience 105:871–879.

Kita H, Kita T, Kitai ST (1985) Active membrane properties of rat neostriatal neurons in an in vitro slice preparation. Exp Brain Res 60:54–62.

Kita H, Kitai ST (1987) Efferent projections of the subthalamic nucleus in the rat: light and electron microscopic analysis with the PHA-L method. J Comp Neurol 260:435–452.

Kolomiets BP, Deniau JM, Glowinski J, Thierry AM (2003) Basal ganglia and processing of cortical information: functional interactions between trans-striatal and trans-subthalamic circuits in the substantia nigra pars reticulata. Neuroscience 117:931–938.

Koos T, Tepper JM (1999) Inhibitory control of neostriatal projection neurons by GABAergic interneurons. Nat Neurosci 2:467–472.

Loucif KC, Wilson CL, Baig R, Lacey MG, Stanford IM (2005) Functional interconnectivity between the globus pallidus and the subthalamic nucleus in the mouse brain slice. J Physiol 567(Pt 3): 977–987.

Maurice N, Deniau JM, Glowinski J, Thierry AM (1999) Relationships between the prefrontal cortex and the basal ganglia in the rat: physiology of the cortico-nigral circuits. J Neurosci 19:4674–4681.

McGeorge AJ, Faull RL (1989) The organization of the projection from the cerebral cortex to the striatum in the rat. Neuroscience 29: 503–537.

Parent A, Hazrati LN (1995) Functional anatomy of the basal ganglia. I. The cortico-basal ganglia-thalamo-cortical loop. Brain Res Rev 20:91–127.

Plenz D, Kitaï ST (1999) A basal ganglia pacemaker formed by the subthalamic nucleus and external globus pallidus. Nature 400: 677–682.

Richards CD, Shiroyama T, Kitai ST (1997) Electrophysiological and immunocytochemical characterization of GABA and dopamine neurons in the substantia nigra of the rat. Neuroscience 80: 545–557.

Romanelli P, Esposito V, Schaal DW, Heit G (2005) Somatotopy in the basal ganglia: experimental and clinical evidence for segregated sensorimotor channels. Brain Res Rev 48:112–128.

Smith Y, Bevan MD, Shink E, Bolam JP (1998) Microcircuitry of the direct and indirect pathways of the basal ganglia. Neuroscience 86:353–387.

Stern EA, Kincaid AE, Wilson CJ (1997) Spontaneous subthreshold membrane potential fluctuations and action potential variability of rat corticostriatal and striatal neurons in vivo. J Neurophysiol 77:1697–1715.

Van der Kooy D, Hattori T, Shannak K, Hornykiewicz O (1981) The pallido-subthalamic projection in rat: anatomical and biochemical studies. Brain Res 204:253–268.

Wilson CJ (1987) Morphology and synaptic connections of crossed corticostriatal neurons in the rat. J Comp Neurol 263:567–580.

Wilson CJ, Groves PM (1981) Spontaneous firing patterns of identified spiny neurons in the rat neostriatum. Brain Res 220:67–80.

(Accepted 3 February 2006)